

Measurement of β -delayed neutrons around the third r -process peak

J.L. Taín, J. Agramunt, A. Algora, F. Molina, I. Mukha, B. Rubio

Instituto de Física Corpuscular, Valencia, Spain

M.B. Gómez-Hornillos, R. Caballero, A. Riego, V. Gorlychev, G. Cortés, C. Pretel, F. Calviño,
A. Poch

Universitat Politècnica de Catalunya, Barcelona, Spain

I. Dillmann, C. Domingo-Pardo, A. Arcones, P. Boutachkov, T. Engert, F. Farinon, H. Geissel,
N. Goel, M. Gorska, M. Heil, R. Hoischen, I. Kojouharov, J. Kurcewicz, J. Marganiec,
G. Martínez-Pinedo, F. Naqvi, C. Nociforo, S. Pietri, R. Plag, R. Reifarth, H. Schaffner,
C. Scheidenberger, H. Weick, J. Winfield, M. Winkler, H.J. Wollersheim

GSI Helmholtzzentrum für Schwerionenforschung GmbH, Darmstadt, Germany

D. Cano-Ott, A. García, T. Martínez

CIEMAT, Madrid, Spain

J. Benlliure, D. Cortina

Universidad de Santiago de Compostela, Spain

W. Gelletly, Z. Podolyak, P. Regan

Department of Physics, University of Surrey, Guildford GU27XH, UK

D. Galaviz-Redondo

CFNUL, Centro de Física Nuclear da Universidade de Lisboa, Portugal

T. Davinson, Z. Liu, P.J. Woods

School of Physics & Astronomy, University of Edinburgh, UK

R.D. Page, P.J. Nolan, T. Grahn

Department of Physics, University of Liverpool, UK

J. Simpson

STFC, Daresbury Laboratory, UK

J.J. Valiente-Dobón, G. de Angelis, E. Sahin, D. Napoli

Laboratori Nazionali di Legnaro, INFN, Italy

D.A. Testov, E. Sokol, Yu. Penionzkevich, V. Smirnov

Flerov Laboratory, Joint Institute for Nuclear Research, Dubna, Russia

T. Kurtukian-Nieto

CENBG - Université Bourdeau 1 - UMR 5797 CNRS/IN2P3, Gradignan Cedex, France

F. Montes, J. Pereira

NSCL, Michigan State University, East Lansing, Michigan, USA

Spokespersons: C. Domingo-Pardo, I. Dillmann, B. Gómez-Hornillos, J.L. Taín

GSI Contact Person: C. Domingo-Pardo.

Abstract

This proposal aims at the measurement of both β -decay half-lives and β -delayed neutron emission probabilities of a number of nuclei near the third r -process peak.

Assuming a ^{238}U beam intensity of 2×10^9 ions per second we have estimated that the isotopes $^{213-216}\text{Tl}$, $^{213,214}\text{Hg}$, $^{208-211}\text{Au}$, $^{208,209}\text{Pt}$ and $^{205,206}\text{Ir}$ can be implanted in sufficient intensity for such studies at the final focal plane of the GSI fragment separator. This will allow, for the first time, the measurement of their β -decay half-lives and neutron emission branching ratios. The high primary beam energy of $1 \text{ GeV}/u$ available at GSI will be crucial for such measurements, in order to avoid contaminations due to incompletely stripped charge states.

The β -delayed neutron emission probability of these isotopes is expected to be at least 5%, and their implantation rates between $\sim 10^{-2} \text{ s}^{-1}$ and 10^{-1} s^{-1} , which should enable their measurement using a high-efficiency neutron detector. The detection system will also include an state-of-the-art array of DSSSDs for the detection of both implanted ions and β -decays. HPGe-detectors will be used for γ -ray tagging and will help for a precise A/q -calibration by measuring isomers in the neighbouring nuclei.

1 Motivation and introduction

The rapid neutron capture process (r process) is characterised by extremely high temperatures of $T \sim 10^9 \text{ K}$ and very large neutron densities of 10^{23} to 10^{30} cm^{-3} . Although the astrophysical site for this process has not been identified yet, it seems clear that it must be related to explosive scenarios such as type II Supernovae [1], where such cataclysmic conditions are presumably encountered. Many of the uncertainties in our understanding of the r process arise from the vast number of neutron-rich nuclei involved (see Fig. 1), where experimental information is rather scarce, uncertain and in most cases non-existent. Provided that the relevant nuclear physics input parameters could be measured with sufficient accuracy, the observed r -process abundance distribution would reflect the history of the r -process nucleosynthesis, its dynamics and the cosmic site or sites where it takes place.

Although the nuclear physics input is rather poorly known it is clear that, the r process shows a prominent influence in the evolution and composition of our Universe, thus it accounts for roughly half of the isotopic abundances observed in the solar system (beyond Iron) and it seems to be the unique mechanism responsible for the existence of the actinide nuclei. Furthermore, nucleochronometry based on the long lived isotopes ^{232}Th and ^{238}U has recently attracted great interest since UV spectroscopy observations made with the Hubble Space Telescope [2], SUBARU [3], Keck-HIRES [4, 5] and the detailed survey from the Hamburg/ESO HERES project [6] revealed the signature of neutron rich heavy elements in ultra metal poor stars, where one can assume that only one single (or few) nucleosynthesis event has contributed to its composition. The age of these ancient stars represents not only a lower limit for the age of the Milky Way Galaxy and of the Universe, but also provides an important constraint on the time of onset of stellar nucleosynthesis, with further implications for galaxy formation and evolution. Radioactive decay ages can be determined by comparing the observed abundances of the Thorium and Uranium elements (relative to a stable r -process element), to the production ratio expected from theoretical r -process yields. Using

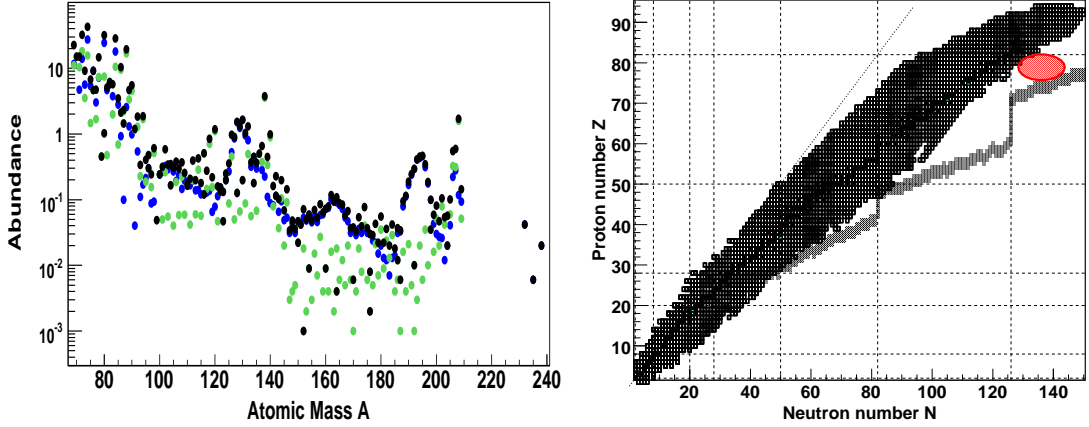


Figure 1: (Left) Solar system abundances (black) and contributions from the s-process (green) and the r-process (blue). (Right) Chart of nuclei showing the r-process path (shaded region) and the region addressed in the present work (red-shaded region).

this approach, stellar ages between 10 Gyr and 17 Gyr are typically obtained, with uncertainties of 3-4 Gyr, which arise in similar proportions from both the nuclear-physics input and the *r*-process model.

The present proposal is aimed at the measurement of β -delayed neutron emission probabilities on several isotopes near the third *r*-process peak. The latter represents the last “bottle-neck” before the synthesis of the heaviest Th and U isotopes, commonly used in cosmochronometry. With the present RIB facilities the nuclei directly involved in this $N \sim 126$ region of the *r*-process path still remain out of the experimentally accessible range. However, by measuring the properties of the neighbouring nuclei one can gain information, which becomes of pivotal importance in order to test and develop theoretical models of relevance for nuclear structure studies and explosive nucleosynthesis.

There have been many β -decay experiments in the region around the first two *r*-process abundance maxima, between $A = 80$ and $A = 130$. Such systematic experiment series have led to a more detailed understanding of the nuclear-structure development towards $N = 82$ and its impact on *r*-process nucleosynthesis [7, 8, 2, 4]. Similarly to the present proposed experiment, β -delayed neutron emission measurements have been carried out in the lower mass region between the first two *r*-process bottlenecks, see e.g. Refs. [9, 10, 11, 12, 13, 14, 15] and in particular close to the *r*-process path along $N = 82$ on the $^{131,132}\text{Cd}$ isotopes [16].

Nevertheless, the experimental information on β -decay studies related to the last *r*-process bottleneck around $N \sim 126$ is very scarce. In this region, recent measurements [17, 18, 19] have provided information of β -decay half-lives for some isotopes. However, no experimental information on β -delayed neutron emission probabilities exists as yet in this region. In this respect, the present proposed experiment is of great relevance for three fundamental reasons: *i*) for the correct interpretation of the *r*-process abundance distribution, especially for the 3rd peak formation (its position, width and height) at $A \sim 195$, *ii*) for the reliable modeling of the last bottle-neck and the further flow of *r*-process matter to Thorium and Uranium and *iii*) for the reliable use of Thorium and Uranium

as cosmo-chronometers in correlation with the nearby 3rd peak and the Pb/Bi-abundances. Indeed, about 80-90% of the *r*-process abundance of the Lead and Bismuth isotopes is due to the decay of the short-lived trans-Bismuth isotopes, which are produced only by the *r* process [20]. For this reason, the *r*-process “residuals” of the Pb/Bi isotopes, obtained by subtracting *s*-process calculated abundances [21] from Solar System abundances, have been commonly used in the past in order to test the performance of *r*-process model calculations in the trans-Bismuth region [20, 8, 22, 22, 23]. However, thanks to the enormous progress on stellar spectroscopic observations [2, 3, 6, 5], the stellar abundances of the 3rd *r*-process peak elements (La, Eu, Er, Hf, and Ir) together with Lead and Bismuth represent nowadays an additional, more complete, and direct test for *r*-process model calculations [24, 4].

In the present proposal we plan to use a primary beam of ^{238}U in order to produce and identify the nuclei $^{213-216}\text{Tl}$, $^{213,214}\text{Hg}$, $^{208-211}\text{Au}$, $^{208,209}\text{Pt}$ and $^{205,206}\text{Ir}$, which neighbour the third *r*-process peak. The unique combination of very high intensity ($2 \times 10^9 \text{ }^{238}\text{U}/\text{s}$) and very high energy (1 GeV/u) available at GSI, will be crucial in order to produce such exotic species in sufficient intensities, and free of contaminant charge states. These very neutron rich isotopes will be implanted at the final focal plane of the GSI fragment separator. We plan to measure, for the first time, their β -decay half-lives and neutron emission branching ratios. Half-lives will be determined, using a state-of-the-art array of DSSSDs, from the time correlations between implantation- and β -decay signals. The β -delayed neutron emission probability will be measured by means of a 4π high efficiency neutron detector [25].

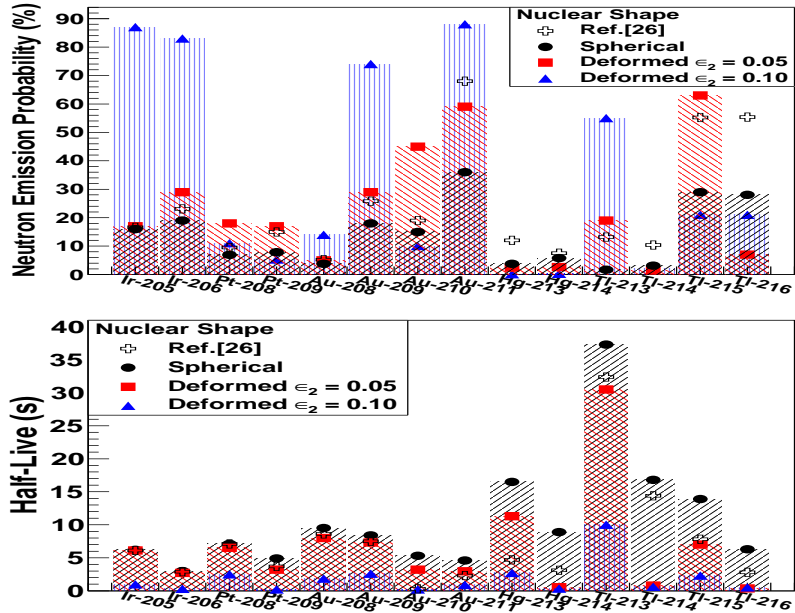


Figure 2: (Top) Calculated [26] neutron emission probabilities, the solid symbols correspond to a new calculation [27] assuming spherical, and deformed ($\varepsilon_2 = 0.05$ and $\varepsilon_2 = 0.10$) nuclear shapes. (Bottom) Same for the half-lives. (See text for details).

β -decay experiments represent a unique opportunity for the study of very neutron-rich nuclei from the nuclear-structure perspective. Indeed, already by comparing the $t_{1/2}$ and P_n measured gross

nuclear properties of the proposed isotopes, a rough insight into the β -strength distribution will be obtained, which reflects the underlying nuclear structure. Such information, very far-off the stability valley, will be an important benchmark for the test and development of nuclear models, and especially for the models commonly used in r -process calculations. According to the Finite-Range Droplet-Model (FRDM), the proposed nuclei are expected to show weakly deformed shapes. This makes the half-lives and P_n values that we plan to measure sensitive to such collectivity effects. Indeed, nuclear deformation affects the relative contributions of Gamow-Teller and first-forbidden transitions, which are reflected in the shape of the β -strength distribution. Figure 2 illustrates the impact of the nuclear deformation in the neutron emission probabilities (top) and in the half-lives (bottom) for all the isotopes proposed in this experiment. The open-cross symbols correspond to the calculation of Ref. [26], which uses the FRDM-mass formula and combines QRPA with the gross theory in order to account for Gamow-Teller and first-forbidden β -decay transitions, respectively. In order to demonstrate the effect of the nuclear deformation, new calculations [27] have been performed for three possible scenarios, of spherical, and slightly deformed ($\varepsilon_2 = 0.05$ and $\varepsilon_2 = 0.10$) shapes (see Fig. 2). In summary, the calculations shown in Fig. 2 serve to illustrate both, the sensitivity of the proposed measurements to nuclear structure effects, and the uncertainties present in the nuclear physics input for r -process calculations.

2 Experiment

For the present experiment one can assume a primary beam intensity of $\sim 2 \times 10^9$ ^{238}U ions per pulse after SIS extraction, with an energy of 1 GeV/u at the production target. Such high primary beam energy will allow also to suppress contaminations due to incompletely stripped charge states. According to LISE++ and MOCADI calculations, a beryllium target with a thickness of about 1.6 g/cm² and equipped with a 223 mg/cm² Nb-stripper will provide the best production rate for the fragments of interest. Degraders with thicknesses of 2 g/cm² and 2 to 4 g/cm² at the first and second FRS focal plane respectively, will allow for an optimal transmission and separation of the secondary fragments. Contaminant charge states will be further suppressed by using slits at the first, second and fourth focal planes. Standard FRS detectors (Scintillators at S2 and S4, MUSIC and TPCs) will be used for ion tracking and identification. An schematic view of the GSI fragment separator FRS is shown in Fig. 3.

The neutron detector in the upgraded version for this experiment will consist of 44 ^3He proportional counters (2.5 cm diameter, 60 cm length at 20 atm) arranged in one inner ring of 12 counters plus two outer rings of 16 counters each (see Fig. 4). The counters are embedded in the polyethylene neutron moderation matrix around the central hole, which accomodates the implantation array of DSSSDs. The system is shielded against external neutrons by additional polyethylene blocks, which reduce this source of background by one order of magnitude. The total size of the ensemble is 90×90×80 cm³. The efficiency response for neutron detection is very flat for energies up to 1 MeV reaching 65% (see Fig. 5). This very high efficiency in combination with the high neutron selectivity of the detector provides a very large sensitivity, thus allowing for the measurement of β -delayed neutron probabilities, even with a small number of counts. A triggerless data acquisition system has been developed [28] in order to register with minimum dead-time and maximum flexibility the β -neutron delayed time correlations.

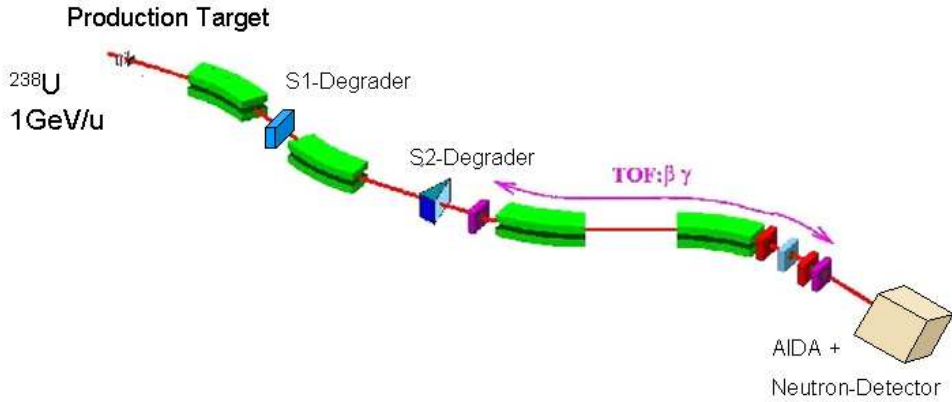


Figure 3: Schematic view of the GSI fragment separator as it is foreseen for the present experiment. At the final focus of the FRS the implantation DSSSDs array in combination with the neutron detector will be used for the measurement of β -decay half-lives and β -delayed neutron emission probabilities.

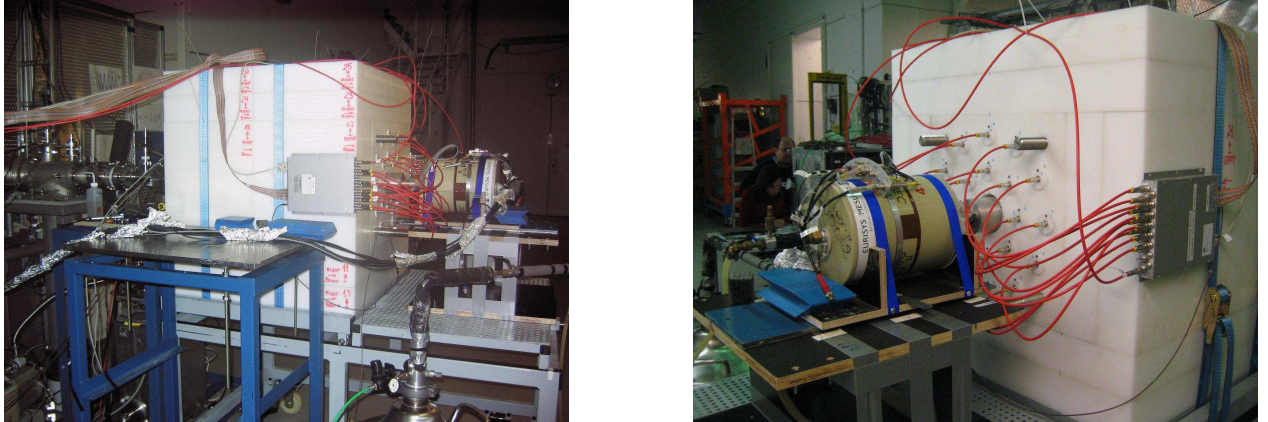


Figure 4: Two views of the neutron detector setup for an experiment at Jyväskylä (in its present version with 20 ^3He counters). For the experiment at GSI the neutron detector will consist of 44 counters (see text) and the semiconductor germanium detector will be replaced by the implantation array of DSSSDs.

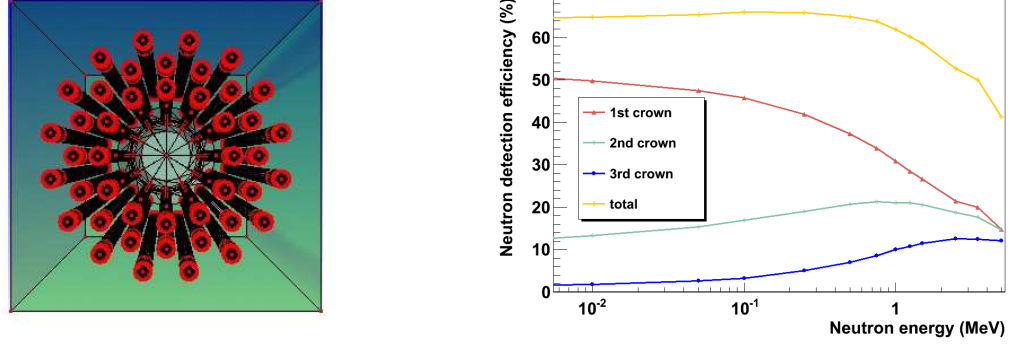


Figure 5: (Left) Schematic view of the neutron detector as it is implemented in the simulation. (Right) Detection efficiency as a function of the neutron energy. The curve shows a parameterisation adjusted to the twelve points simulated with the MCNPX code.

To illustrate the experimental accessibility of the proposed nuclei, the FRS intensities calculated for a representative setting of ^{216}Tl and the neutron emission probabilities [26] are displayed in Fig. 6. Clearly, a large area of β -delayed neutron emitting isotopes is illuminated with relatively high FRS-intensities. As shown later, the isotopes of Thallium and Gold are excellent candidates for the present experiment.

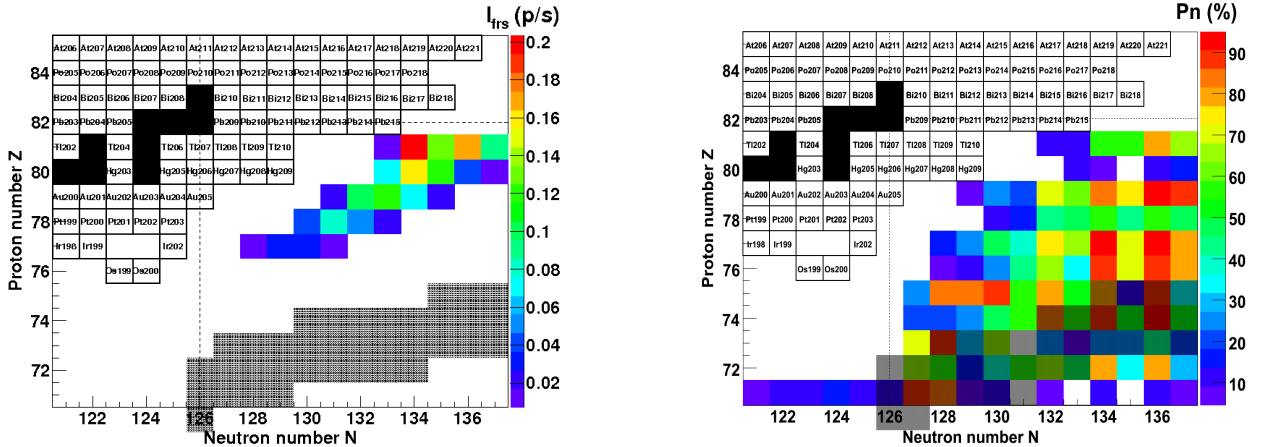


Figure 6: (Left) Chart of nuclei in the region ‘north-east’ of the precursors of the 3rd r -process peak. The displayed isotopic intensities correspond to an FRS-setting on ^{216}Tl . (Right) Expected β -delayed neutron emission probabilities [26] for several nuclei in the region of interest. The grey-shaded region shows the r -process path. Note the lower cut of 5% in the right diagram.

In some particular cases, depending on the neutron-emission yields of the neighbouring nuclei, it becomes more convenient to use a cleaner beam by cutting-off as much as possible the surrounding

isotopes. Indeed, contaminations due to neutrons emitted by nuclei with similar A/q -values may represent an important source of background. In such cases, the FRS parameters will be set for the nucleus of interest, and the neighbouring nuclei will be highly suppressed by operating the FRS in achromatic mode and with the help of the collimation slits and a rather dispersive degrader (about 4 g/cm²) at the second FRS focal plane S2. The drawback of the energy gradient connected with the achromatic beam will be counterbalanced by the large number of highly pixeleted DSSSD implantation detectors. In this way, production rates can be optimised, while keeping the spatial implantation distributions rather clean and the total beam-time within reasonable limits.

Table 1: List of nuclei of interest and the calculated implantation rates (2nd col). Expected neutron emission probabilities [26], β -decay half-lives [26], neutron detection rates and total number of detected neutrons are listed in columns 3 to 6. The last column indicates which FRS-settings contribute significantly to the production of the nucleus of interest listed in the first column. See text for the beam-time requested for each FRS-setting.

Nucleus of Interest	Rate (p/s)	P _n (%)	t _{1/2} (s)	C _{βn} (counts/s)	C _{βn} × Δt (counts)	FRS-Setting(s)
²¹³ Tl	0.15	13.2	32.4	4.8×10 ⁻³	416	²¹⁴ Hg+ ²¹¹ Au
²¹⁴ Tl	0.32	10.4	14.4	8.1×10 ⁻³	700	²¹⁶ Tl+ ²¹⁴ Hg+ ²¹¹ Au
²¹⁵ Tl	0.24	55.2	7.8	3.2×10 ⁻²	2800	²¹⁶ Tl+ ²¹⁴ Hg+ ²¹¹ Au
²¹⁶ Tl	5.5×10 ⁻²	55.4	2.8	7.3×10 ⁻³	634	²¹⁶ Tl
²¹³ Hg	7.3×10 ⁻²	12.0	4.7	2.1×10 ⁻³	181	²¹⁴ Hg+ ²⁰⁹ Pt
²¹⁴ Hg	3.5×10 ⁻²	7.5	3.1	6.3×10 ⁻⁴	54	²¹⁴ Hg+ ²⁰⁹ Pt
²⁰⁸ Au	4.4×10 ⁻²	5.2	8.6	5.5×10 ⁻⁴	95	²⁰⁹ Pt
²⁰⁹ Au	9.4×10 ⁻²	25.8	7.5	5.8×10 ⁻³	1006	²¹¹ Au+ ²⁰⁹ Pt
²¹⁰ Au	5.1×10 ⁻²	19	0.3	2.3×10 ⁻³	400	²¹¹ Au
²¹¹ Au	2.6×10 ⁻²	68	2.3	4.3×10 ⁻³	745	²¹¹ Au
²⁰⁸ Pt	2.0×10 ⁻²	9.5	7.1	4.6×10 ⁻⁴	40	²⁰⁹ Pt
²⁰⁹ Pt	1.2×10 ⁻²	15	3.7	4.2×10 ⁻⁴	36	²⁰⁹ Pt
²⁰⁵ Ir	1.5×10 ⁻²	16.6	6.1	6.0×10 ⁻⁴	52	²⁰⁶ Ir
²⁰⁶ Ir	8.6×10 ⁻³	23.1	2.9	4.8×10 ⁻⁴	41	²⁰⁶ Ir

The expected count-rates listed in Table 1 are based on P_n-values calculated using the FRDM-mass model and they include both Gamow-Teller and first-forbidden β -decay transitions [26]. Starting from those isotopes which show calculated neutron emission probabilities [26] larger than 5% we have performed a systematic study using LISE++ and MOCADI in order to estimate the implantation rates ion-by-ion. These calculations include the newest cross section values available, which combine the recent modification of the abration-ablation model ABRABLA [29] with the COFRA model [30]. The nuclei of interest (Table 1) can be produced in sufficient intensities by means of the following five FRS-settings: ²¹⁶Tl (1 day), ²¹⁴Hg (1 day), ²¹¹Au (2 days), ²⁰⁹Pt (1 day) and ²⁰⁶Ir (1 day). The expected detection count-rates and total statistics for the quoted beam-time are summarized in Table 1. In these calculations we have assumed rather conservative values for the efficiency of both the neutron detector (60%) and the implantation array (40%). The latter will consist of either an

state-of-the-art stack of 3-5 highly segmented DSSSDs or a prototype of the AIDA detector [31]. The half-lives of the proposed nuclei will be determined from the time correlation between implantation- and β -decay signals, following the approach described in Ref. [32].

3 Beam time request

Although the calculated beam intensities and the neutron emission probabilities are relatively large, from the FRS point of view this experiment is highly demanding due to the complexity of the region of the chart of nuclides to be accessed and the large number of FRS-settings. Therefore we ask for 1 day of FRS calibration, 1 day to account for the FRS setup time elapsed between measurements, and 6 days for the complete measurement. The total beam time requested is therefore 8 days.

References

- [1] J. J. Cowan and F.-K. Thielemann. R-Process Nucleosynthesis in Supernovae. *Physics Today*, 57(10):100000–53, October 2004.
- [2] J.J. Cowan *et al.* Hubble Space Telescope Observations of Heavy Elements in Metal-Poor Galactic Halo Stars. *The Astrophysical Journal*, 627:238–250, July 2005.
- [3] N. Tominaga *et al.* Population III Core-Collapse Supernova Yields and Extremely Metal-Poor Star Abundance Pattern. In S. Kubono, W. Aoki, T. Kajino, T. Motobayashi, & K. Nomoto, editor, *Origin of Matter and Evolution of Galaxies*, volume 847 of *American Institute of Physics Conference Series*, pages 488–490, July 2006.
- [4] I.U. Roederer *et al.* The End of Nucleosynthesis: Production of Lead and Thorium in the Early Galaxy. *The Astrophysical Journal*, 698:1963–1980, June 2009.
- [5] A. Frebel *et al.* High-Resolution Spectroscopy of Extremely Metal-Poor Stars in the Least Evolved Galaxies: Ursa Major II and Coma Berenices. *The Astrophysical Journal*, 708:560–583, January 2010.
- [6] W. Hayek *et al.* The Hamburg/ESO R-process enhanced star survey (HERES). IV. Detailed abundance analysis and age dating of the strongly r-process enhanced stars CS 29491-069 and HE 1219-0312. *Astronomy & Astrophysics*, 504:511–524, September 2009.
- [7] K.L. Kratz *et al.* Nuclear structure studies at ISOLDE and their impact on the astrophysical r-process. *Hyperfine Interactions*, 129:185–221, December 2000.
- [8] H. Schatz *et al.* Thorium and Uranium Chronometers Applied to CS 31082-001. *The Astrophysical Journal*, 579:626–638, November 2002.
- [9] H. Ohm *et al.* Beta-delayed neutrons and high-energy gamma-rays from decay of ^{137}I . *Zeitschrift fur Physik A Hadrons and Nuclei*, 296:23–33, March 1980.

- [10] K.-L. Kratz *et al.* Observation of beta-delayed neutron decay to excited 0^+ states in the residual nucleus: The case $^{97}\text{Rb}(\beta\text{n}\gamma)^{96}\text{Sr}$. *Physics Letters B*, 103:305–308, July 1981.
- [11] H. Gabelmann *et al.* P_n -values of short-lived Sr, Y, Ba and La precursors. *Zeitschrift fur Physik A Hadrons and Nuclei*, 308:359–360, December 1982.
- [12] K.-L. Kratz *et al.* Beta-delayed neutron emission from $^{93-100}\text{Rb}$ to excited states in the residual Sr isotopes. *Zeitschrift fur Physik A Hadrons and Nuclei*, 306:239–257, September 1982.
- [13] J.C. Wang *et al.* β -delayed neutron decay of ^{104}Y , ^{112}Tc , ^{113}Tc and ^{114}Tc : test of half-life predictions for neutron-rich isotopes of refractory elements. *Physics Letters B*, 454:1–7, May 1999.
- [14] F. Montes *et al.* β -decay half-lives and β -delayed neutron emission probabilities for neutron rich nuclei close to the N=82r-process path. *Physical Review C*, 73(3):035801, March 2006.
- [15] J. Pereira *et al.* β -decay half-lives and β -delayed neutron emission probabilities of nuclei in the region $A < 110$, relevant for the r process. *Physical Review C*, 79(3):035806, March 2009.
- [16] M. Hannawald *et al.* Selective laser ionization of very neutron-rich cadmium isotopes: Decay properties of $^{131}\text{Cd}_{83}$ and $^{132}\text{Cd}_{84}$. *Physical Review C*, 62(5):054301, November 2000.
- [17] T. Kurtukian. *Production and β decay half-lives of heavy neutron-rich nuclei approaching the stellar nucleosynthesis r-process path around $A=195$* . PhD thesis, Universidade de Santiago de Compostela, 2007.
- [18] T. Kurtukian-Nieto *et al.* Recent progress in measuring β half-lives of nuclei approaching the r-process waiting point $A = 195$. *Nuclear Physics A*, 827:587–589, August 2009.
- [19] T. Kurtukian-Nieto, *et al.*, 2010. Submitted for publication to Phys. Rev. Lett.
- [20] J.J. Cowan *et al.* R-Process Abundances and Chronometers in Metal-poor Stars. *The Astrophysical Journal*, 521:194–205, August 1999.
- [21] C. Arlandini *et al.* Neutron Capture in Low-Mass Asymptotic Giant Branch Stars: Cross Sections and Abundance Signatures. *The Astrophysical Journal*, 525:886–900, November 1999.
- [22] C. Domingo-Pardo *et al.* Resonance capture cross section of Pb207. *Physical Review C*, 74(5):055802, November 2006.
- [23] C. Domingo-Pardo *et al.* Measurement of the radiative neutron capture cross section of Pb206 and its astrophysical implications. *Physical Review C*, 76(4):045805, October 2007.
- [24] K.-L. Kratz *et al.* Explorations of the r-Processes: Comparisons between Calculations and Observations of Low-Metallicity Stars. *The Astrophysical Journal*, 662:39–52, June 2007.
- [25] M.B. Gómez-Hornillos *et al.* A 4π neutron detector for beta-delayed neutron emission studies. *Nuclear Instruments and Methods in Physics Research A*, 2010. (in preparation).
- [26] P. Möller *et al.* New calculations of gross β -decay properties for astrophysical applications: Speeding-up the classical r process. *Physical Review C*, 67(5):055802, May 2003.

- [27] K.-L. Kratz (private communication).
- [28] J. Agramunt *et al.* A triggerless digital data acquisition system for beta-decay experiments. *Nuclear Instruments and Methods in Physics Research A*. (in preparation).
- [29] K.-H. Schmidt *et al.* Fission of nuclei far from stability. *Nuclear Physics A*, 693:169–189, October 2001.
- [30] J. Benlliure. Production of neutron-rich isotopes by cold fragmentation in the reaction $^{197}\text{Au} + \text{Be}$ at 950 A MeV. *Nuclear Physics A*, 660:87–100, December 1999.
- [31] D. Braga *et al.* AIDA: a 16-Channel Amplifier ASIC to Read Out the Advanced Implantation Detector Array for Experiments in Nuclear Decay Spectroscopy. *IEEE Transactions in Nuclear Science (submitted)*, 2009.
- [32] T. Kurtukian-Nieto *et al.* A new analysis method to determine β -decay half-lives in experiments with complex background. *Nuclear Instruments and Methods in Physics Research A*, 589:472–483, May 2008.